Contribution from the Department of Chemistry,
University of Houston, Houston, Texas 77004

Chloride-Binding Reactions and Electrochemistry of (TPP)Co^{II} and (TPP)Co^{III}Cl in Dichloromethane

K. M. Kadish,* X. Q. Lin, and B. C. Han

Received February 13, 1987

The electrochemistry of (tetraphenylporphinato)cobalt(II), (TPP)Co, and chloro(tetraphenylporphinato)cobalt(III), (TPP)Co^{III}Cl, is reported in methylene chloride solutions containing various concentrations of tetrabutylammonium chloride. The two-electron reduction of (TPP)Co^{III}Cl or the one-electron reduction of (TPP)Co generates [(TPP)Co^{I}]$^-$, but these reversible electroreductions are followed by a rapid irreversible chemical reaction with the CH_2Cl_2 solvent to produce a σ-bonded cobalt(III) complex. Electrooxidation of (TPP)Co in the presence of Cl^- generates either (TPP)Co^{III}Cl or [(TPP)Co^{III}Cl$_2$]$^-$ after abstraction of one electron and [(TPP)Co^{III}Cl]$^+$ or (TPP)Co^{III}Cl$_2$ after abstraction of a second electron. The [(TPP)Co^{II}Cl]$^-$/[(TPP)Co^{III}Cl$_2$]$^-$ and [(TPP)Co^{III}Cl$_2$]$^-$/(TPP)Co^{III}Cl$_2$ reactions occur at E_p = 0.57 V (cyclic voltammetry, scan rate = 0.1 V/s) and $E_{1/2}$ = 0.63 V, respectively. (TPP)Co^{III}Cl is reversibly oxidized to [(TPP)Co^{III}Cl]$^+$ at 0.90 V and to [(TPP)Co^{III}Cl]$^{2+}$ at 1.15 V in the absence of excess Cl^-. ESR, UV–visible, and thin-layer spectroelectrochemical methods were utilized to characterize the reactants and products of each electrode reaction, and a mechanism for the chloride-binding reactions and electrochemistry of (TPP)Co and (TPP)Co^{III}Cl is presented.

Introduction

Numerous reports of cobalt porphyrin electrochemistry have appeared in the literature.[1-16] Half-wave potentials for the oxidation or reduction of (P)Co (where P = the dianion of a given porphyrin ring) depend upon the coordination number of both Co(III) and Co(II) and vary substantially with changes in the solvent/supporting electrolyte mixtures.[1] The first oxidation of (TPP)Co in dry CH_2Cl_2 involves formation of a Co(II) cation radical[7] while the second and third oxidations involve abstraction of electrons first from the Co(II) center and then from the porphyrin π ring system. This ordering in the site of electron transfer is reversed in potentially coordinating solvents or in the presence of nucleophiles where the first oxidation of (P)Co invariably involves the Co(II)/Co(III) transition.

Values of $E_{1/2}$ and the site of electron abstraction for the first oxidation of (P)Co are extremely sensitive to the presence of coordinating ligands. A negative shift in $E_{1/2}$ of approximately 1.0 V[1] occurs upon changing the solvent from dry methylene chloride where the reaction is porphyrin ring centered to pyridine where the reaction is metal centered. Negative shifts in potential for Co(II)/Co(III) also occur upon coordination with other neutral solvent molecules, but under these conditions the second and third oxidations of (TPP)Co shift in a positive direction.[3,4]

The two reductions of (P)Co result in formation of [(P)Co^{I}]$^-$ and [(P)Co^{I}]$^{2-}$. These reactions have been well characterized in nonaqueous solvents such as DMF or Me_2SO[3,4,8,15] and occur at $E_{1/2}$ values in the range of -0.85 ± 0.05 and -1.80 ± 0.05 V vs. SCE. The electrogenerated [(P)Co^{I}]$^-$ is stable in most media, and the spectroscopic properties of isolated Na[(TPP)Co^{I}]·5THF have been reported.[17] However, if alkyl or aryl halides are added to solutions of [(P)Co^{I}]$^-$, a reaction occurs that leads to the formation of (P)Co(R).[10] In fact, one common method for synthesizing σ-bonded cobalt porphyrins is to react chemically or electrochemically generated [(P)Co^{I}]$^-$ with RX.[9,11,18-21]

The electrochemical and chemical oxidations of cobalt porphyrins have been extensively investigated with respect to the site of electron abstraction (central metal or π ring system) and the spectroscopic properties of the oxidized complex. Neutral and oxidized cobalt(III) porphyrins have been characterized by ESR,[12,23,24,26,27] NMR,[5,22] and resonance Raman[22] spectroscopy. Special attention has been devoted to (TPP)Co^{III}Cl, which can be activated in solution to form six-coordinate Co(III) π cation radicals.[23,24,26,27]

Chemically and electrochemically generated π cation radicals of cobalt(III) porphyrins have also been investigated with respect to their molecular structure and electronic state.[23,24,28,29] The HOMO of the cation radical has been identified as an a_{2u} π orbital, and a spin-polarization mechanism of ρ_N^{π} has been suggested to explain the observed ^{59}Co hyperfine shifts.[24]

Very little data exists as to how complexed halide ions affect the potentials and mechanisms for oxidation and reduction of (TPP)Co. A ring-centered oxidation of (TPP)Co^{III}X, where X = Cl^-, Br^-, I^-, PF_6^-, or ClO_4^-, has been reported to occur at 0.600 V vs. SCE at a Hg electrode in methylene chloride.[5] This potential is close to the limit for oxidation of Hg and is within the range of potentials reported for the metal-centered oxidation of (TPP)Co

(1) Kadish, K. M. *Prog. Inorg. Chem.* **1986**, *34*, 435.
(2) Lin, X. Q.; Boisselier-Cocolios, B.; Kadish, K. M. *Inorg. Chem.* **1986**, *25*, 3242.
(3) Walker, F. A.; Beroiz, D.; Kadish, K. M. *J. Am. Chem. Soc.* **1976**, *98*, 3484.
(4) Truxillo, L. A.; Davis, D. G. *Anal. Chem.* **1975**, *47*, 2260.
(5) Huet, J.; Gaudemer, A.; Boucly-Goester, C.; Boucly, P. *Inorg. Chem.* **1982**, *21*, 3413.
(6) Lin, X. Q.; Kadish, K. M. *Anal. Chem.* **1985**, *57*, 1498.
(7) Fajer, J., private communication.
(8) Kadish, K. M.; Bottomley, L. A.; Beroiz, D. *Inorg. Chem.* **1978**, *17*, 1124.
(9) Dolphin, D.; Halko, D. J.; Johnson, E. *Inorg. Chem.* **1981**, *20*, 4348.
(10) Lexa, D.; Savéant, J.-M.; Soufflet, J. P. *J. Electroanal. Chem. Interfacial Electrochem.* **1979**, *100*, 159.
(11) Perree-Fauvet, M.; Gaudemer, A.; Boucly, P.; Devynck, J. *J. Organomet. Chem.* **1976**, *120*, 439.
(12) Wolberg, A.; Manassen, J. *J. Am. Chem. Soc.* **1970**, *92*, 2982.
(13) Wolberg, A. *Isr. J. Chem.* **1974**, *12*, 1031.
(14) Callot, H. J.; Cromer, R.; Louati, A.; Gross, M. *Nouv. J. Chim.* **1984**, *8*, 765.
(15) Felton, R. H.; Linschitz, H. *J. Am. Chem. Soc.* **1966**, *88*, 1113.
(16) Momenteau, M.; Lexa, D. *Biochem. Biophys. Res. Commun.* **1974**, *58*, 940.
(17) Kobayashi, H.; Hara, T.; Kaizu, Y. *Bull. Chem. Soc. Jpn.* **1972**, *45*, 2148.
(18) Clarke, D. A.; Dolphin, D.; Grigg, R.; Johnson, A. W.; Pinnock, H. A. *J. Chem. Soc.* **1968**, 881.
(19) Clarke, D. A.; Grigg, R.; Johnson, A. W.; Pinnock, H. A. *J. Chem. Soc., Chem. Commun.* **1967**, 305.
(20) Ogoshi, H.; Watanabe, E.; Koketsu, N.; Yoshida, Z. *Bull. Chem. Soc. Jpn.* **1976**, *49*, 2529.
(21) Momenteau, M.; Fournier, M.; Rougee, M. *J. Chim. Phys.* **1970**, *67*, 926.
(22) Yamamoto, K.; Uzawa, J.; Chizimatsu, T. *Chem. Lett.* **1979**, 89.
(23) Ohya-Nishiguchi, H.; Khono, M.; Yamomoto, K. *Bull. Chem. Soc. Jpn.* **1981**, *54*, 1923.
(24) Ichimori, K.; Ohya-Nishiguchi, H.; Hirota, N.; Yamomoto, K. *Bull. Chem. Soc. Jpn.* **1985**, *58*, 623.
(25) Sakurai, T.; Yamamoto, K.; Naito, H.; Nakamoto, N. *Bull. Chem. Soc. Jpn.* **1976**, *49*, 3042.
(26) Yamamoto, K.; Konno, M.; Ohya-Nishiguchi, H. *Chem. Lett.* **1981**, 255.
(27) Yamamoto, K.; Hoshino, M.; Kohno, M.; Ohya-Nishiguchi, H. *Bull. Chem. Soc. Jpn.* **1986**, *59*, 351.
(28) Dolphin, D.; Forman, A.; Borg, D. C.; Fajer, J.; Felton, R. H. *Proc. Natl. Acad. Sci. U.S.A.* **1971**, *68*, 614.
(29) Dolphin, D.; Muljiani, Z.; Rousseau, K.; Borg, D. C.; Fajer, J.; Felton, R. H. *Ann. N.Y. Acad. Sci.* **1973**, *206*, 177.

0020-1669/87/1326-4161$01.50/0

at a Pt electrode in CH_2Cl_2 containing different (TBA)X supporting electrolytes. For example, the first oxidation of (TPP)Co is reported to occur at $E_{1/2}$ = 0.74 V vs. SCE in CH_2Cl_2 containing 0.1 M (TBA)Cl and at $E_{1/2}$ = 0.29 V vs. SCE in CH_2Cl_2 containing 0.1 M (TBA)Br.[4]

In this paper, we report the electrochemistry of (TPP)Co and (TPP)Co^{III}Cl in CH_2Cl_2 with and without excess chloride ions. The one-electron reduction of (TPP)Co or the two-electron reduction of (TPP)Co^{III}Cl yields [(TPP)Co^{I}]$^-$, but these reversible electrochemical reactions are followed by an irreversible chemical reaction involving CH_2Cl_2 that produces a σ-bonded cobalt complex. Both thin-layer and bulk ESR/UV–visible spectroelectrochemical techniques were used to characterize each electrode reaction, and an overall oxidation/reduction mechanism is presented.

Experimental Section

Instrumentation. Conventional and thin-layer cyclic voltammograms were obtained with a PAR Model 174A polarographic analyzer or an IBM Model ED 225 voltammetric analyzer and an Omnigraphic 2000 X-Y recorder using a three-electrode system. The working electrode for conventional voltammetry was a platinum button with surface area of about 0.8 mm^2. A homemade saturated calomel electrode (SCE) served as the reference electrode and was separated from the bulk solution by an asbestos-tipped glass frit which also functioned as a Luggin capillary to reduce *iR* drop. An expanded platinum electrode with about a 1 mm^2 surface area was used as the auxiliary electrode. High-purity nitrogen was used to remove any oxygen from the bulk solution and to maintain a N_2 atmosphere above the solution during the experiment.

Electrochemically monitored chloride titrations of (TPP)Co were carried out in a Vacuum Atmosphere Model 43-2 Dri-Lab with a Model HE-493 Dri-Train system. Spectroelectrochemical experiments were carried out with a vacuum-tight short-path-length thin-layer spectroelectrochemical cell, which utilizes a doublet platinum-gauze working electrode.[6] A Tracor Northern TN-1710 multichannel analyzer was combined with a TN-1710-24 floppy disk system for spectral data acquisitions.

Thin-layer spectroelectrochemical ESR experiments were conducted with an IBM ER 100D spectrometer and a specially designed thin-layer quartz ESR cell. This cell has a thin-layer chamber with dimensions of 22 × 3.5 × 0.5 mm^3 and was vertically placed in the center of the TE_{102} microwave cavity. An expanded platinum-metal working electrode of 15 × 3 × 0.3 mm^3 was inserted into the thin-layer chamber, which was open to the bulk solution at both the upper and lower ends. Two expanded platinum-metal auxiliary electrodes were placed at each end of the thin-layer cell to reduce *iR* drop.

In order to minimize interferences from the electrogenerated species, the two auxiliary electrodes were positioned 5 cm away from the thin-layer chamber. The cell volume was about 10 mL, but only about 0.4% of the solution was electrolyzed in each experiment. An aqueous SCE electrode was used as the reference electrode, which was placed in a asbestos-tipped glass frit. The tip of the reference frit was placed in the thin-layer chamber to further reduce *iR* drop.[30] In this way well-defined thin-layer cyclic voltammograms could be obtained in the ESR cavity.

Chemicals. (TPP)Co and (TPP)Co^{III}Cl were synthesized and characterized according to methods described in the literature.[5,25] Spectroscopic grade methylene chloride (CH_2Cl_2) (Fisher Scientific Co.) was freshly distilled from CaH_2 before use. Tetrabutylammonium perchlorate (TBAP) (Fluka Chemical Co.) was recrystallized twice from ethanol and dried in vacuo prior to use. Tetrabutylammonium chloride ((TBA)Cl) (Fluka) was dried under N_2 with 10-Å molecular sieves in ethanol and recrystallized from the ethanol solution under reduced pressure. The purified compounds were dried under vacuum and stored in the Dri-Lab.

Electrochemically Monitored Chloride Titrations. Changes in chloride coordination upon oxidation or reduction of (TPP)Co were determined by shifts in half-wave potential as a function of the Cl^- concentration.[31] Both the bulk solution and the frit solution had the same initial ionic strength and were simultaneously titrated.

Results and Discussion

Electroreduction of (TPP)Co. The first reduction of (TPP)Co is reversible in CH_2Cl_2 at scan rates greater than 1.0 V/s and corresponds to the reaction (TPP)Co^{II} + e^- ⇄ [(TPP)Co^{I}]$^-$. However, the electrogenerated [(TPP)Co^{I}]$^-$ is not stable and

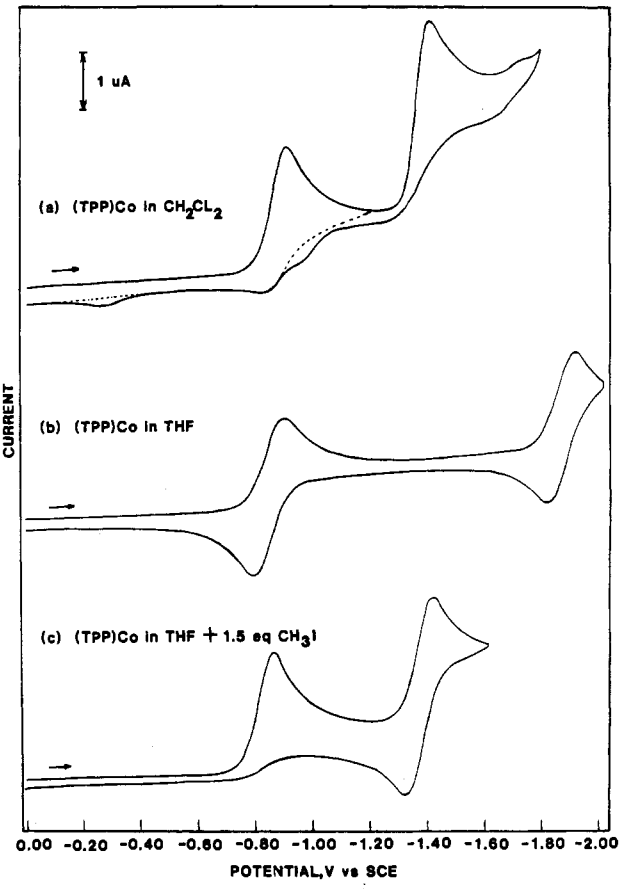

Figure 1. Cyclic voltammograms of (a) (TPP)Co in CH_2Cl_2, 0.1 M TBAP; (b) (TPP)Co in THF, 0.1 M TBAP; and (c) (TPP)Co in THF, 0.1 M TBAP, plus 1.5 equiv of CH_3I. Scan rate = 0.10 V/s.

rapidly reacts with CH_2Cl_2. This is evident at slower potential scan rates and leads to a voltammogram such as that shown in Figure 1a. When the potential scan is terminated at −1.20 V the first reduction at E_{pc} = −0.91 V is coupled to a reoxidation peak at E_{pa} = −0.84 V (dashed line, Figure 1a). However, if the potential is scanned to more negative values, there are two additional anodic peaks at E_{pa} = −0.97 and −0.28 V. There is also an irreversible process at E_{pc} = −1.40 V. This peak is not observed in other nonaqueous solvents[1,3,4] which have voltammograms similar to the one illustrated in THF (Figure 1b).

Currents for the second reduction of (TPP)Co in CH_2Cl_2 are higher than those for the first reduction, and the peak potential for this process is within experimental error of potentials for the reduction of (TPP)Co(CH_3) in CH_2Cl_2.[32] This suggests the formation of (TPP)Co(CH_2Cl) from a reaction involving [(TPP)Co^{I}]$^-$ and CH_2Cl_2. The formation of (TPP)Co(R) from chemically or electrochemically generated [(TPP)Co^{I}]$^-$ and RX is well-known[9,11,18-21] but has never been demonstrated to occur on the cyclic voltammetry time scale in CH_2Cl_2.

The irreversible nature of the first and second (TPP)Co reduction in CH_2Cl_2 suggests the sequence of electrode reactions shown in Scheme I.

Scheme I

$$(TPP)Co^{II} + e^- \rightleftarrows [(TPP)Co^{I}]^-$$

$$[(TPP)Co^{I}]^- + CH_2Cl_2 \rightarrow (TPP)Co(CH_2Cl) + Cl^-$$

$$(TPP)Co(CH_2Cl) \overset{e^-}{\rightleftarrows} [(TPP)Co(CH_2Cl)]^- \xrightarrow[-CH_2Cl]{} \text{products}$$

$$(TPP)Co^{II} \overset{e^-}{\rightleftarrows} [(TPP)Co^{I}]^-$$

(30) Lin, X. Q.; Kadish, K. M. *Anal. Chem.* **1986**, *58*, 1493.
(31) Kadish, K. M. In *Iron Porphyrins, Part 2*; Lever, A. B. P., Gray, H. B., Eds.; Addison-Wesley: Reading, MA, 1983; pp 161–249.
(32) (TPP)Co(CH_3) is reduced to [(TPP)Co(CH_3)]$^-$ at $E_{1/2}$ = −1.42 V in CH_2Cl_2, 0.1 M TBAP, and at $E_{1/2}$ = −1.39 V in THF, 0.1 M TBAP.

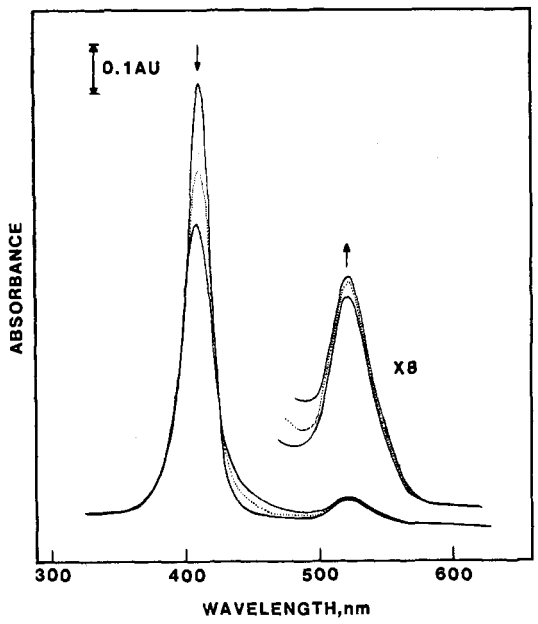

Figure 2. Thin-layer spectral changes during the controlled-potential reduction of (TPP)Co at −1.2 V vs. SCE in CH_2Cl_2, 0.1 M TBAP.

Table I. Half-Wave and Peak Potentials (V vs. SCE) for Oxidation and Reduction of (TPP)Co and (TPP)Co^{III}Cl in CH_2Cl_2 Containing 0.1 M TBAP/(TBA)Cl Mixtures

initial compd	concn of (TBA)Cl	$E_{1/2}$	$E_{1/2}$	$E_{1/2}$ or E_p[a]
(TPP)Co^{III}Cl	0	1.15	0.90	E_{pa} = 0.57 E_{pc} = 0.20
(TPP)Co^{II}	0	1.16	0.97	0.78
	1.1 equiv	1.19	0.92	E_{pa} = 0.57 E_{pc} = 0.20
	2.2 equiv	1.13	0.63	E_{pa} = 0.57 E_{pc} = 0.18
	180 equiv		0.69	E_{pa} = 0.33 E_{pc} = 0.10
	0.1 M[b]			0.74
	0.1 M		0.68	E_{pa} = 0.28 E_{pc} = 0.15

[a] Values obtained at a scan rate of 0.10 V/s. [b] From ref 4.

Thin-layer spectra were taken during the first controlled-potential reduction of (TPP)Co and are illustrated in Figure 2. The final spectral product after the addition of one electron has absorption bands at 408 and 524 nm and is similar to spectra of (TPP)Co(CH_3) (408 and 530 nm) and (TPP)Co(C_2H_5) (407 and 524 nm)[9] in CH_2Cl_2. Other (TPP)Co(R) complexes where R = a phenyl or substituted phenyl group have also been spectrally characterized in CH_2Cl_2.[33] The Soret bands of these complexes range between 408 and 419 nm while the visible bands are located between 529 and 534 nm. These spectral data are summarized in Table II, which also lists spectra for electrogenerated [(TPP)Co^I]$^-$ in THF. Electrogenerated [(TPP)Co^I]$^-$ in THF has a split Soret band at 365 and 424 nm and a visible band at 509 nm. These absorptions agree with literature spectra[17] of [(TPP)Co^I]$^-$ and are similar in PhCN, THF, Me_2SO, and pyridine.[34]

The overall reactions in Scheme I involve a catalytic reduction of the halogenated hydrocarbon, which in this case is CH_2Cl_2. This type of reaction is well-known in cobalt porphyrin chemistry[10] and is similar to reactions reported for the reduction of rhodium(III) porphyrins in the same solvent.[35]

The reduction of (TPP)Co(R) to first give [(TPP)Co(R)]$^-$ followed by [(TPP)Co^I]$^-$ formation has been characterized in Me_2SO,[11] and this reaction also seems to occur in CH_2Cl_2. There is no evidence of [(TPP)Co(CH_2Cl)]$^-$ oxidation on the reverse scan in CH_2Cl_2, thus suggesting that a rapid cleavage of the cobalt–carbon bond has occurred. The electrogenerated [(TPP)Co^I]$^-$ can then react further with CH_2Cl_2 or it may be reoxidized back to (TPP)Co^{II} or [(TPP)Co^{II}Cl]$^-$ on the reverse negative scan.

Table II. Spectral Properties of [(TPP)Co^I]$^-$ and (TPP)Co(R) Complexes

species	solvent	λ_{max}, nm ($10^{-4}\epsilon$)			ref
[(TPP)Co^I]$^-$	THF	365 (7.2)	424 (9.4)	509 (1.4)	c
(TPP)Co(CH_3)	CH_2Cl_2		408 (12.4)	530 (0.7)	c
(TPP)Co(C_2H_5)	CH_2Cl_2		407	524	9
(TPP)Co(CH_2Cl)[a]	CH_2Cl_2		408 (19.2)	524 (1.9)	c
(TPP)Co(CH_2Cl)[b]	CH_2Cl_2/2 equiv of Cl^-		409 (21.0)	529 (1.9)	c

[a] Generated by electroreduction of (TPP)Co in CH_2Cl_2, 0.1 M TBAP. [b] Generated by electroreduction of (TPP)Co in CH_2Cl_2, 0.1 M TBAP and 2 equiv of (TBA)Cl. [c] This work.

Scheme II

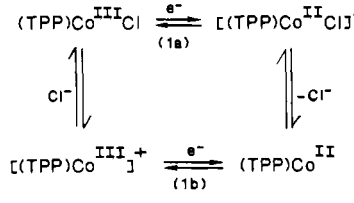

The voltammogram for reduction of (TPP)Co in CH_2Cl_2 is similar to voltammograms of (TPP)Co in nonaqueous solvents containing excess RX. An example is shown in parts b and c of Figure 1, which illustrate the reduction of (TPP)Co in THF with and without added CH_3I. Reversible reductions of (TPP)Co are observed at $E_{1/2}$ = −0.85 and −1.86 V in the absence of CH_3I. Small concentrations of CH_3I were then added to the solution, and this led to a voltammogram of the type shown in Figure 1c. This latter voltammogram is characterized by an irreversible peak at E_{pc} = −0.86 V and a reversible peak at $E_{1/2}$ = −1.39 V. The currents for the two reduction processes are approximately equal, consistent with the stability of the singly reduced [(TPP)Co(CH_3)]$^-$ and the one-electron transfer in each step.

Electrochemistry of (TPP)Co^{III}Cl. A cyclic voltammogram of (TPP)Co^{III}Cl in CH_2Cl_2 containing 0.1 M TBAP is shown in Figure 3. The reversible oxidations at $E_{1/2}$ = 0.90 and 1.15 V are labeled as processes 2′ and 3′ and correspond to the two ring oxidations of the Co(III) complex. The first reduction of (TPP)Co^{III}Cl has noncoupled cathodic and anodic peaks, which are labeled as peak 1a (reduction) and peak 1b (oxidation) and were spectroelectrochemically characterized as involving a Co(III)/Co(II) transition. The reduction of (TPP)Co^{III}Cl (peak 1a) occurs at E_p = 0.20 V at a scan rate of 0.10 V/s while a reoxidation of the generated Co(II) complex (peak 1b) occurs at E_p = 0.57 V at the same scan rate.

A second reduction of (TPP)Co^{III}Cl occurs at E_{pc} = −0.90 V. This reduction (process 4′) involves the Co(II)/Co(I) transition and shows characteristics of a coupled chemical reaction when the potential scan rate was less than 1 V/s. Under these conditions a third reduction at E_p = −1.42 V is observed. This process (process 5) involves the reduction of electrogenerated (TPP)Co(CH_2Cl) and has been discussed in the previous section.

The noncoupled Co(III)/Co(II) reactions of (TPP)Co^{III}Cl can be explained by the "box mechanism" shown in Scheme II. In this scheme the reduction and reoxidation of (TPP)Co^{III}Cl occur via two separate reversible electron-transfer steps, each of which is coupled to a following chemical reaction.

The one-electron reduction of (TPP)Co^{III}Cl generates a transient [(TPP)Co^{II}Cl]$^-$ species before loss of Cl^- (overall process 1a). The generated (TPP)Co^{II} can then be reoxidized to [(TPP)Co^{III}]$^+$, but this oxidation is followed by a rapid binding of Cl^- to regenerate (TPP)Co^{III}Cl (overall process 1b). This box mechanism is not unusual[1] and has been shown to occur for

(33) Callot, H. J.; Metz, F.; Cromer, R. *Nouv. J. Chim.* **1984**, *8*, 759.
(34) Kadish, K. M.; Mu, X. H., manuscript in preparation.
(35) Anderson, J. E.; Yao, C.-L.; Kadish, K. M. *Inorg. Chem.* **1986**, *25*, 718.

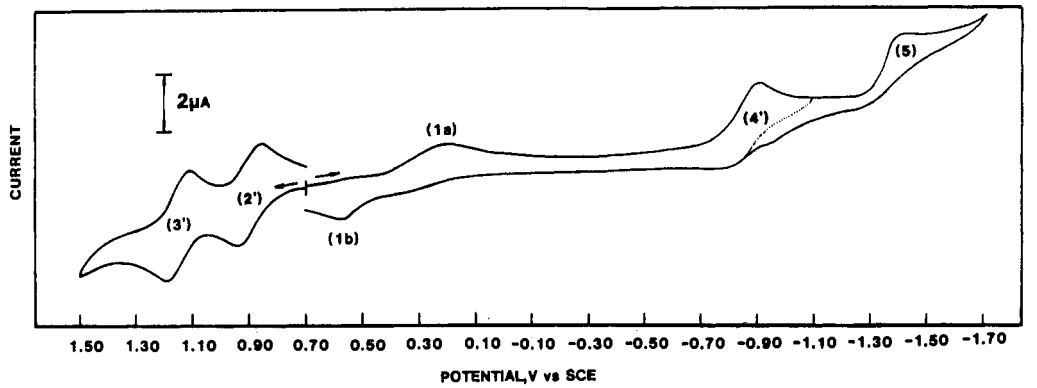

Figure 3. Cyclic voltammogram of (TPP)$Co^{III}Cl$ at a platinum electrode in CH_2Cl_2, 0.1 M TBAP, at a scan rate of 0.10 V/s.

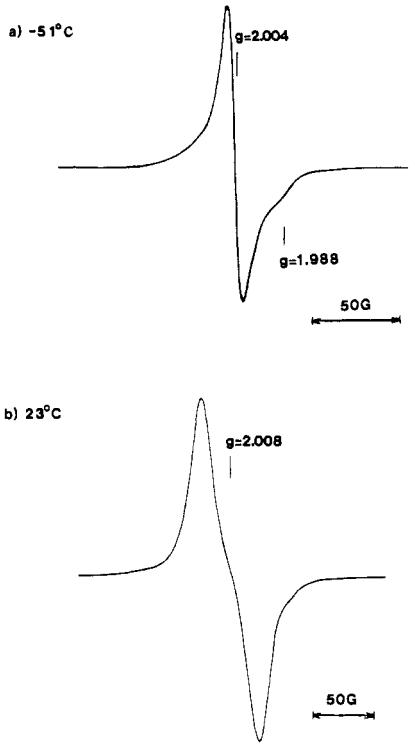

Figure 4. ESR spectrum of (TPP)$Co^{III}Cl$ after electrolysis at 1.1 V vs. SCE in CH_2Cl_2 containing 0.1 M TBAP at (a) −51 °C and (b) 23 °C.

(TPP)FeCl,[36] (TPP)MnCl,[37] and (TPP)CrCl.[38]

The second and third oxidations of (TPP)$Co^{III}Cl$ are well-defined and correspond to the reactions shown in eq 1 and 2.

$$(TPP)Co^{III}Cl \rightleftarrows [(TPP)Co^{III}Cl]^+ + e^- \quad (1)$$

$$[(TPP)Co^{III}Cl]^+ \rightleftarrows [(TPP)Co^{III}Cl]^{2+} + e^- \quad (2)$$

Reaction 1 involves formation of a Co(III) cation radical while reaction 2 involves formation of the Co(III) dication. Each of the positively charged species has an associated anion, which can be either ClO_4^- or Cl^-, resulting from a disproportionation reaction. This is discussed in the following sections.

Temperature-Dependent ESR of $[(TPP)Co^{III}Cl]^+$. Bulk electrolysis of (TPP)$Co^{III}Cl$ at 1.1 V vs SCE in CH_2Cl_2 containing 0.1 M TBAP solution gives a strong ESR signal at both room and low temperatures. These ESR spectra are shown in Figure 4. The low-temperature signal of $[(TPP)Co^{III}Cl]^+$ (Figure 4a) is slightly asymmetric with $g_\perp = 2.004$ and $g_\parallel = 1.988$. This signal is not identical with the cation radical signals of $[(TPP)Co^{III}]^+$[2,23,24] and

Table III. ESR Parameters of $[(TPP)Co^{III}]^{2+}$ π Cation Radicals in CH_2Cl_2, 0.1 M TBAP

species	T, °C	g (±0.002)	ΔH,[a] G	ref
$[(TPP)Co^{III}]^{2+}$	23	2.003	42	*c*
	−70	2.003	37.7	23
	−70	2.003	44	24
	−150	2.004	37	*c*
$[(TPP)Co^{III}Cl]^+$	18	2.008	47	*c*
	−51	2.004/1.988[b]		*c*
	−70	2.005	49	23
(TPP)$Co^{III}Cl_2$	23	2.004	87	*c*
	−40	2.003	80	26
	−70	2.003	80	23
	−150	2.003	74	*c*

[a] Total peak-to-peak width including hfcc. [b] $g_\perp > g_\parallel$. [c] This work.

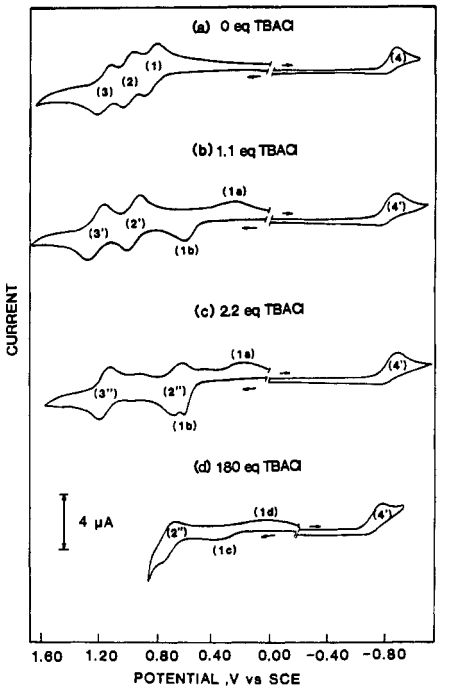

Figure 5. Cyclic voltammograms of 4.7×10^{-4} M (TPP)Co in CH_2Cl_2 solution containing 0.1 M TBAP/(TBA)Cl mixtures at 100 mV/s.

(TPP)$Co^{III}Cl_2$.[23,24,26] However, after approximately 30 min of continued controlled-potential electrolysis, the ESR signal changed so that it became similar to the radical signal of (TPP)$Co^{III}Cl_2$. This may be due to the decomposition of CH_2Cl_2 during prolonged electrolysis, which resulted in trace Cl^- in solution. (TPP)$Co^{III}Cl_2$ may also be formed from a disproportionation involving (TPP)-$Co^{III}Cl$. This is discussed in later sections of the paper.

The signals shown in Figure 4 are assigned as the π-cation radical of (TPP)$Co^{III}Cl$. The HOMO of symmetric (TPP)CoX_2

(36) Bottomley, L. A.; Kadish, K. M. *Inorg. Chem.* **1981**, *20*, 1348.
(37) Kadish, K. M.; Kelly, S. *Inorg. Chem.* **1979**, *18*, 2968.
(38) Bottomley, L. A.; Kadish, K. M. *Inorg. Chem.* **1983**, *22*, 342.

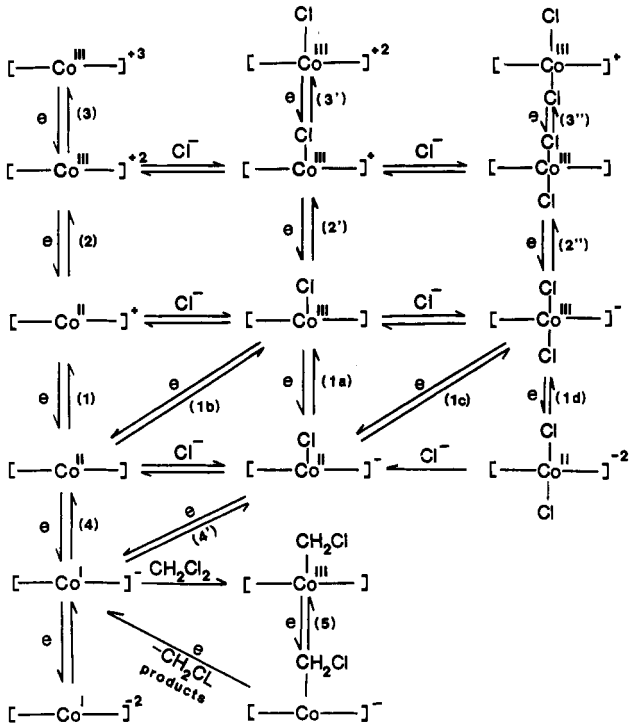

Figure 6. Overall oxidation/reduction scheme for (TPP)Co and (TPP)Co^{III}Cl in CH_2Cl_2 with and without excess Cl^-.

has been determined to be a_{2u} and D_{4h}[24] and the singly occupied molecular orbital (HOMO) of $[(TPP)Co^{III}Cl]^+$ is not significantly different than other Co(III) a_{2u} radicals which have small splitting constants.

The ESR spectrum of electrooxidized (TPP)Co^{III}Cl is temperature dependent. At room temperature the signal is located at $g = 2.008$ and has a peak-to-peak width of 47 G (see Figure 4b). This signal is also different from the cation radical signal of $[(TPP)Co^{III}]^{2+}$ and (TPP)Co$^{III}Cl_2$. Parameters of these cation radicals are summarized in Table III.

Electrochemically Monitored Titration of (TPP)Co with Chloride. Figure 5 shows cyclic voltammograms of (TPP)Co in CH_2Cl_2 containing 0.1 M TBAP and increasing concentrations of (TBA)Cl. In the absence of (TBA)Cl there are three reversible oxidations at $E_{1/2}$ = 0.78, 0.97, and 1.16 V vs. SCE and two reductions at E_{pc} = −0.88 V and E_{pc} = −1.42 V vs. SCE. The reversible oxidations are labeled processes 1, 2, and 3 in Figure 5a while the first reduction is labeled as process 4. The first reduction (process 4) does not shift from E_p = −0.88 V during the titration. However, as (TBA)Cl is added to solution, the first oxidation transition (process 1) shifts to more negative potentials and shows noncoupled reduction/reoxidation peaks that are labeled as peaks 1a and 1b. The two ring-centered oxidations (processes 2 and 3) also shift to more negative potentials with increase in chloride ion concentration while the difference in $E_{1/2}$ between these two reactions becomes larger. This is shown in Figure 5b, which is the cyclic voltammogram of (TPP)Co in the presence of 1.1 equiv (TBA)Cl. This cyclic voltammogram is identical with that of (TPP)Co^{III}Cl in CH_2Cl_2 (see Figure 3), and under these conditions the two reversible oxidations are labeled as peaks 2′ and 3′. The electrode reactions are given by eq 1 and 2.

Further additions of (TBA)Cl result in the voltammograms such as those shown in Figure 5c,d. The oxidation/reduction peaks of process 2 continue to shift negatively until they reach a constant value around $E_{1/2}$ = 0.63 V. This occurs after 2.0 equiv of Cl^- has been added to solution. Under these conditions the oxidation peaks of (TPP)Co are labeled as 2″ and 3″. Peak 1b also shifts negatively between 1 and 3 equiv of (TBA)Cl, after which point no further shifts in E_p are noted. This peak then decreases in intensity with increasing concentration of Cl^- and finally disappears in CH_2Cl_2 solutions containing about 60 equiv of chloride ion have been added.

Scheme III

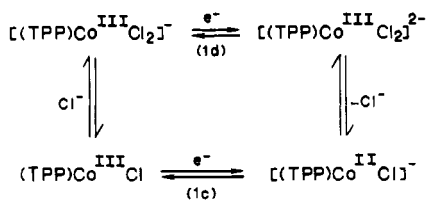

A broad oxidation peak occurs at 0.38 V in CH_2Cl_2 containing 60 equiv of (TBA)Cl (~0.03 M). This peak shifts negatively with further increases of chloride concentration and is coupled to a broad rereduction peak at 0.1 V, which shifts negatively, however, to 0.0 V when the (TBA)Cl concentration is increased to 180 equiv (0.075 M). The half-wave and peak potentials of each electrode reaction were measured as a function of the (TBA)Cl formal concentration, and an overall mechanism for (TPP)Co and (TPP)Co^{III}Cl oxidation/reduction consistent with these data is shown in Figure 6.

The potentials for each oxidation/reduction reaction of (TPP)Co and (TPP)Co^{III}Cl under various conditions are listed in Table I. In the absence of Cl^- the three oxidations occur at 0.78, 0.97, and 1.16 V and are represented by reactions 1–3. (TPP)Co^{III}Cl is oxidized to $[(TPP)Co^{III}Cl]^+$ and $[(TPP)Co^{III}Cl]^{+2}$ (eq 1 and 2) and these oxidations are given by reactions 2′ and 3′ in Figures 5 and 6. Electrooxidation of $[(TPP)Co^{III}Cl_2]^-$ generates (TPP)Co$^{III}Cl_2$ and $[(TPP)Co^{III}Cl_2]^+$, and these reactions are labeled as 2″ and 3″ in Figures 5 and 6.

The Co(II)/Co(III) oxidation/reduction proceeds by noncoupled reactions at all concentrations of Cl^-. In the case of (TPP)Co^{III}Cl, the mechanism is as shown in Scheme II, and under these conditions, the anodic and cathodic peaks are labeled as reactions 1a (reduction) and 1b (oxidation). A similar box scheme occurs for reduction and reoxidation of $[(TPP)Co^{III}Cl_2]^-$. These reactions are given in Scheme III. Under these conditions the reduction of bis-ligated Co(III) to bis-ligated Co(II) is given by peak 1d while that for oxidation of mono-ligated Co(II) to mono-ligated Co(III) is given by peak 1c. Both reactions are coupled to following chemical reactions that involve the loss of Cl^- from $[(TPP)Co^{III}Cl_2]^{2-}$ or the addition of Cl^- to (TPP)Co^{III}Cl.

The reduction of (TPP)Co (reaction 4, Figure 6) or $[(TPP)Co^{II}Cl]^-$ (reaction 4′, Figure 6) invariably leads to the same σ-bonded Co(III) species, which is assigned as (TPP)Co(CH_2Cl). This complex can be reduced to form $[(TPP)Co(CH_2Cl)]^-$ (reaction 5, Figure 6), but this product is not stable in CH_2Cl_2 and a further electron transfer occurs that is accompanied by cleavage of the cobalt–carbon bond and regeneration of $[(TPP)Co^I]^-$.

Spectroelectrochemical Characterization of Electrogenerated $[(TPP)Co^{III}Cl_2]^-$ and (TPP)Co$^{III}Cl_2$. The first two oxidations of (TPP)Co in CH_2Cl_2 solutions containing 2 equiv of (TBA)Cl were characterized by thin-layer spectroelectrochemistry. These spectral changes are shown in Figure 7 and Table IV and correspond to the electrochemical generation of $[(TPP)Co^{III}Cl_2]^-$ and (TPP)Co$^{III}Cl_2$ after the successive abstraction of two electrons.

The first spectral changes occur as the potential is scanned from 0.20 to 0.53 V. The characteristic Soret band of $[(TPP)Co^{II}Cl]^-$ at 410 nm completely disappears during this process, and a newly formed Soret band of $[(TPP)Co^{III}Cl_2]^-$ appears at 443 nm. In the visible region, the single $[(TPP)Co^{II}Cl]^-$ band at 529 nm disappears as the bands at 558 and 598 nm for $[(TPP)Co^{III}Cl_2]^-$ are formed. A set of well-defined isosbestic points is observed at 376, 425, 507, and 545 nm, indicating the rapid addition of Cl^- to electrochemically generated (TPP)Co^{III}Cl to give the final $[(TPP)Co^{III}Cl_2]^-$ product.

The oxidation of $[(TPP)Co^{III}Cl_2]^-$ occurs at $E_{1/2}$ = 0.63 V (see Figure 5), and additional spectral changes are obtained during a potential scan from 0.53 to 0.72 V. These spectra are shown in Figure 7b, which illustrates the formation of (TPP)Co$^{III}Cl_2$ from $[(TPP)Co^{III}Cl_2]^-$. Upon oxidation, the Soret band of $[(TPP)Co^{III}Cl_2]^-$ at 443 nm decreases dramatically as new absorption bands of (TPP)Co$^{III}Cl_2$ form at 366, 421, and 442 nm. The $[(TPP)Co^{III}Cl_2]^-$ bands at 558 and 598 nm also disappear and

Table IV. Spectral Characteristics of Cobalt(II) and Cobalt(III) Porphyrins in CH_2Cl_2, 0.1 M TBAP

cobalt oxidn state	absorbing species	λ, nm ($10^{-4}\epsilon$, cm^{-1} M^{-1})				
Co(II)	(TPP)Co	410 (29.5)	528 (1.6)			
	$[(TPP)Co^{II}Cl]^-$ [a]	410 (28.9)	529 (1.5)			
1e oxidn	$[(TPP)Co^{II}]^+$ [c]	427 (19.3)	540 (1.92)			
	$(TPP)Co^{III}Cl$ [b]	406 (11.2)	544 (1.32)	900 (0.033)		
	$[(TPP)Co^{III}Cl_2]^-$ [a]	443 (18.1)	558 (1.03)	598 (0.49)		
2e oxidn	$[(TPP)Co^{III}]^{2+}$	415 (9.72)	455 (3.57)	597 (1.15)	662 (1.08)	
	$(TPP)Co^{III}Cl_2$ [a]	366 (2.35)	421 (6.46)	442 (6.42)	595 (0.74)	684 (0.54)
3e oxidn	$[(TPP)Co^{III}]^{3+}$	352 (3.58)	417 (3.03)	455 (1.08)	564 (0.98)	

[a] In CH_2Cl_2, 0.1 M TBAP, plus 2 equiv of (TBA)Cl. [b] Yamamoto, K.; Kohno, M.; Ohya-Nishiguchi, H. *Bull. Chem. Soc. Jpn.* **1986**, *59*, 351–354. [c] Species assigned as a cobalt(II) porphyrin cation radical.[7]

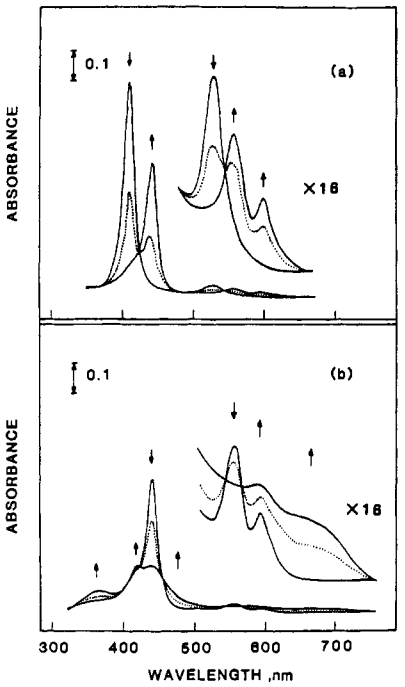

Figure 7. Thin-layer spectral changes during oxidation of (TPP)Co in CH_2Cl_2 containing 0.1 M TBAP and 2 equiv of (TBA)Cl. The potential was scanned at 2 mV/s (a) from 0.20 to 0.53 V to generate $[(TPP)Co^{III}Cl_2]^-$ and (b) from 0.53 to 0.72 V to generate the $(TPP)Co^{III}Cl_2$ cation radical.

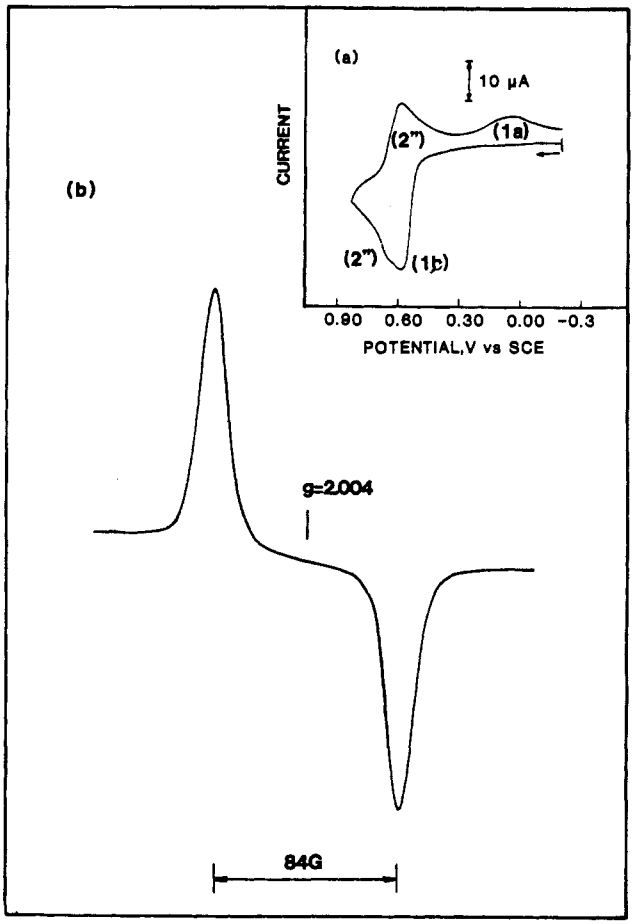

Figure 8. (a) Thin-layer cyclic voltammogram and (b) thin-layer room-temperature ESR spectrum after oxidation of (TPP)Co at 0.75 V in CH_2Cl_2, 0.1 M TBAP, containing 2 equiv of (TBA)Cl.

are replaced by broad absorptions of $(TPP)Co^{III}Cl_2$ in the 500–750-nm region (see Figure 7b). A set of well-defined isobestic points is found at 425, 455, 552, and 565 nm. Table IV summarizes the spectral characteristics of $(TPP)Co^{III}Cl_2$ as well as other cobalt(III) porphyrin cation radicals in the presence and absence of Cl^-.

Spectral changes during the reduction of (TPP)Co in CH_2Cl_2 containing 2 equiv of (TBA)Cl are listed in Table II. The Soret band of (TPP)Co at 410 nm decreases slighly and shifts to 409 nm during the addition of one electron while the Q-band at 529 nm remains invariant. The final spectrum is almost identical with that observed after reduction of (TPP)Co in the absence of excess Cl^- (see Figure 2 and Table II) and is assigned as due to the formation of $(TPP)Co(CH_2Cl)$.

ESR Studies of Electrochemically Generated $(TPP)Co^{III}Cl_2$. Figure 8a shows a cyclic voltammogram of (TPP)Co in the thin-layer ESR–electrochemical cell containing CH_2Cl_2 and 2 equiv of (TBA)Cl. Under these conditions the cobalt(II) complex exists as $[(TPP)Co^{II}Cl]^-$. The first two oxidation steps of $[(TPP)Co^{II}Cl]^-$ (processes 1b and 2", Figure 8a) overlap, but the rereduction process occurs in two separate steps (processes 2" and 1a, Figure 8a). The voltammogram in this thin-layer cell is similar to the conventional cyclic voltammogram shown in Figure 5 and indicates that a well-controlled electrode potential is obtained in the thin-layer ESR cell.

$[(TPP)Co^{II}Cl]^-$ does not show a room-temperature ESR signal in well-deoxygenated solutions, but a radical signal appears during potential scans from 0.5 V to 0.9 V. The signal obtained at 0.75 V is shown in Figure 8b and is identical with that reported in the literature[23,24,26] for $(TPP)Co^{III}Cl_2$. Bulk electrolysis of $[(TPP)Co^{II}Cl]^-$ was also carried out at 0.75 V and showed temperature-dependent signals suggested as due to $(TPP)Co^{III}Cl_2$. These ESR parameters are summarized in Table III.

Disproportionation of $(TPP)Co^{III}Cl$. The reported[22-24] paramagnetic properties of $(TPP)Co^{III}Cl$ might arise from a disproportionation reaction that generates $[(TPP)Co^{III}Cl]^+$ and $[(TPP)Co^{II}Cl]^-$. The $E_{1/2}$ for $[(TPP)Co^{III}Cl]^+$ formation from $(TPP)Co^{III}Cl$ (reaction 2', Figure 6) is 0.90 V while $(TPP)Co^{III}Cl$ reduction (reaction 1a, Figure 6) occurs at E_{pc} = 0.20 V in CH_2Cl_2. Thus, the disproportion constant K_{eq} can be calculated as 9.6×10^{-12} for reaction 3. This indicates that a minimal

$$2(TPP)Co^{III}Cl \rightleftarrows [(TPP)Co^{III}Cl]^+ + [(TPP)Co^{II}Cl]^- \quad (3)$$

amount of $[(TPP)Co^{III}Cl]^+$ and $[(TPP)Co^{II}Cl]^-$ will be generated from the disproportionation.

The cation radical experimentally detected from solutions of $(TPP)Co^{III}Cl$ was not $[(TPP)Co^{III}Cl]^+$ but rather was (TPP)-

$Co^{III}Cl_2$.[23,24,26] It is possible that the disproportionation reaction is combined with chloride anion transformation as shown in reaction 4. The binding of a second chloride ion to the Co(III)

$$2(TPP)Co^{III}Cl \rightleftarrows (TPP)Co^{III}Cl_2 + (TPP)Co^{II} \quad (4)$$

center significantly reduces the $E_{1/2}$ for cation radical formation which occurs at 0.63 V as shown in Figure 5. The equilibrium constant for reaction 4 can thus be estimated as 3.6×10^{-7}. This corresponds to 0.12% species existing in either the cation radical state or the paramagnetic Co(II) state of the compound. A similar mechanism for the paramagnetic properties of $(TPP)Co^{III}Cl$ has also been suggested.[5]

Acknowledgment. The support of the National Science Foundation (Grant No. CHE-8515411) is gratefully acknowledged. We also acknowledge Pierre-F. Blanchet for preliminary electrochemical results on reactions involving formation of (P)-Co(CH_2Cl).

Registry No. (TPP)Co, 14172-90-8; $[(TPP)Co]^-$, 31886-96-1; $[(TPP)Co]^+$, 38414-01-6; $[(TPP)Co]^{2+}$, 28132-69-6; $[(TPP)Co]^{3+}$, 60430-19-5; (TPP)CoCl, 60166-10-1; $[(TPP)CoCl]^-$, 109123-05-9; $[(TPP)CoCl]^+$, 109123-04-8; $(TPP)CoCl_2$, 78992-04-8; $[(TPP)CoCl_2]^-$, 109123-07-1; $(TPP)Co(CH_3)$, 29130-60-7; $[(TPP)Co(CH_3)]^-$, 109123-06-0; $(TPP)Co(CH_2Cl)$, 65856-25-9; Bu_4NCl, 1112-67-0; Cl, 16887-00-6; Bu_4NClO_4, 1923-70-2.

Contribution from the Department of Chemistry, University of Houston, Houston, Texas 77004, and Laboratoire de Synthèse et d'Electrosynthèse Organométallique, Associé aux CNRS (UA 33), Faculté des Sciences "Gabriel", Université de Dijon, 21100 Dijon, France

Synthesis, Electrochemistry, and Ligand-Addition Reactions of Gallium(III) Porphyrins

K. M. Kadish,*[1a] J.-L. Cornillon,[1a] A. Coutsolelos,[1b] and R. Guilard*[1b]

Received March 2, 1987

The synthesis, electrochemistry, and ligand-addition reactions of ionic five- and six-coordinate gallium(III) porphyrins are reported. The reactions of *N*-methylimidazole and pyridine with (P)GaX, where P = the dianion of octaethylporphyrin (OEP) or tetraphenylporphyrin (TPP) and X = Cl^-, OAc^-, OH^-, or F^-, were monitored by ^1H NMR, electrochemistry, electronic absorption spectroscopy, and conductivity measurements. Results from all four methods were self-consistent and demonstrated the stepwise formation of hexacoordinated gallium porphyrin species of the type (P)GaX(L) and $[(P)Ga(L)_2]^+$ where L = *N*-methylimidazole or pyridine. This is the first time that monomeric, hexacoordinated Ga(III) porphyrins have been reported. Equilibrium constants for ligand binding by (P)GaX and (P)GaX(L) were calculated from the electronic absorption spectra, and an overall oxidation/reduction mechanism is presented.

Introduction

It has been demonstrated that cofacially joined organometallic macrocyclic polymers such as $[M(Pc)O]_n$ (where M = Si, Ge, or Sn and Pc = the dianion of phthalocyanine) give stable conducting materials after being partially oxidized with a variety of reagents.[2-8] The isoelectronic group 13 polymers $[(Pc)AlF]_n$ and $[(Pc)GaF]_n$ can also be partially oxidized with I_2[9] or nitrosyl salts,[10,11] and the resulting materials are highly conducting.

Variation of the central metal and the anionic bridging ligand in partially oxidized $[(Pc)MX]_n$ structures may provide valuable insight into how in-plane ring spacing affects the electronic and optical properties of the complex. This was demonstrated for the case of partially oxidized $[(Pc)GaX]_n$ and $[(Pc)AlX]_n$, where X^- = Cl^-, Br^-, or I^-. The resulting complexes were partially oxidized with nitrosyl salts and had a high conductivity.[4]

Variation of the macrocyclic ligand in the polymer may also lead to insights as to how the properties of the macrocycle affect the conducting properties of the complex, and the preparation of various precursors is of interest. In this regard, the synthesis[12] and characterization of gallium σ-bonded alkyl- and arylporphyrins and the bridge-stacked polymeric structure[13] of a complex containing fluorinated gallium(III) porphyrins have been published. The properties of the oxidized polymer are obviously related to the electrochemistry of the monomeric material, and the electrochemistry of σ-bonded gallium(III) porphyrins has also been published.[14]

This present article focuses on the synthesis, electrochemistry, and ligand-addition reactions of five- or six-coordinate gallium(III) porphyrins containing ionic axial ligands. The investigated complexes are represented by (P)GaX or (P)GaX(L), where P is the dianion of tetraphenylporphyrin (TPP) or octaethylporphyrin (OEP), X = Cl^-, OAc^-, OH^-, or F^-, and L = H_2O. Some of these metalloporphyrins may be precursors for conductors, and it is thus of importance to have knowledge concerning the electrochemical properties and ligand-addition reactions of these monomeric complexes. The ligand-addition reactions were monitored by ^1H NMR and UV–visible spectroscopy, conductimetry, and electrochemistry.

Experimental Section

Instrumentation. Electronic absorption spectra were taken by using a Perkin-Elmer 559 spectrophotometer, a Tracor Northern 1710 holographic optical spectrometer/multichannel analyzer, or an IBM 9430 spectrophotometer. IR spectra were obtained on a Perkin-Elmer 1330 spectrometer or a Perkin-Elmer 580B spectrometer. Samples were 1% dispersions in CsI or Nujol mulls. ESR spectra were recorded on an IBM Model ER 100D spectrometer equipped with an ER 40-X microwave bridge and an ER 080 power supply. ^1H NMR spectra were obtained on a Nicolet FT 300 or a JEOL FX-100 spectrometer. Samples were typically 3–4 mg in 0.5 mL of solvent, which was CD_2Cl_2, $CDCl_3$, C_6D_6, or pyridine-d_5. Mass spectra were recorded in the electron-impact mode on a Finnigan 3300 spectrometer. All spectra were obtained by direct inlet under the following conditions: electron impact; ionizing energy, 35–70 eV; ionizing current, 0.4 mA; source temperature, up to 250 °C.

Cyclic voltammograms were obtained with a three-electrode system. The working electrode was a platinum button and the counterelectrode a platinum wire. A saturated calomel electrode (SCE) served as a reference electrode and was separated from the bulk of the solution by a fritted glass bridge. An EG&G Model 173 potentiostat, an EG&G Model 175 universal programmer, and a Houston Instruments Model 200

(1) (a) University of Houston, (b) Université de Dijon.
(2) Nohr, R. S.; Kuznesof, P. M.; Wynne, K. J.; Kenney, M. E.; Siebenmann, P. G. *J. Am. Chem. Soc.* **1981**, *103*, 4371.
(3) Diel, B. N.; Inabe, T.; Lyding, J. W.; Schoch, K. F.; Kannewurf, C. R.; Marks, T. J. *J. Am. Chem. Soc.* **1983**, *105*, 1539.
(4) Nohr, R. S.; Wynne, K. J. *J. Chem. Soc., Chem. Commun.* **1981**, 1210.
(5) Swift, D. R. Ph.D. Dissertation, Case Western Reserve University, 1970.
(6) Kroenke, W. J.; Sutton, L. E.; Joyner, R. D.; Kenney, M. E. *Inorg. Chem.* **1963**, *2*, 1064.
(7) Esposito, J. N.; Lloyd, J. E.; Kenney, M. E. *Inorg. Chem.* **1966**, *5*, 1979.
(8) Linsky, J. P.; Paul, T. R.; Nohr, R. S.; Kenney, M. E. *Inorg. Chem.* **1980**, *19*, 3131.
(9) Petersen, J. L.; Schramm, C. S.; Stojakovic, D. R.; Hoffman, B. M.; Marks, T. J. *J. Am. Chem. Soc.* **1977**, *99*, 286.
(10) Brant, P.; Nohr, R. S.; Wynne, K. J.; Weber, D. *Mol. Cryst. Liq. Cryst.* **1982**, *81*, 255.
(11) Weber, D. C.; Brant, P.; Nohr, R. S.; Haupt, S. G.; Wynne, K. J. *J. Phys., Colloq. C-3* **1983**, *44*, *Suppl. No. 6*, 639.
(12) Coutsolelos, A.; Guilard, R. *J. Organomet. Chem.* **1983**, *253*, 273.
(13) Goulon, J.; Friant, P.; Goulon-Ginet, C.; Coutsolelos, A.; Guilard, R. *Chem. Phys.* **1984**, *83*, 367.
(14) Kadish, K. M.; Boisselier-Cocolios, B.; Coutsolelos, A.; Mitaine, P.; Guilard, R. *Inorg. Chem.* **1985**, *24*, 4521.

0020-1669/87/1326-4167$01.50/0